

Long dephasing time and high-temperature conductance fluctuations in an open InGaAs quantum dot

B. Hackens,¹ F. Delfosse,¹ S. Faniel,¹ C. Gustin,¹ H. Boutry,¹ X. Wallart,² S. Bollaert,² A. Cappy,² and V. Bayot¹

¹CERMIN, PCPM, and DICE Labs, Université Catholique de Louvain, B-1348 Louvain-la-Neuve, Belgium

²IEMN, Cité Scientifique, Villeneuve d'Ascq, France

(Received 4 October 2002; published 19 December 2002)

We measure the electron phase-coherence time τ_ϕ up to 18 K using universal fluctuations in the low-temperature magnetoconductance of an open InGaAs quantum dot. The temperature dependence of τ_ϕ is *quantitatively* consistent with the two-dimensional model of electron-electron interactions in disordered systems. In our sample, τ_ϕ is two to four times larger than previously reported in GaAs quantum dots. We attribute this enhancement to a larger value of the Fermi energy and the lower electron effective mass in our sample. We also observe a distinct type of conductance fluctuation due to ballistic electron focusing inside the dot up to 204 K.

DOI: 10.1103/PhysRevB.66.241305

PACS number(s): 73.23.-b, 73.23.Ad, 73.63.Kv

Since the pioneering work of Marcus and co-workers,¹ open ballistic quantum dots (QDs) have mainly been used as tools to investigate two main issues: ballistic electron dynamics and electron decoherence. When their mean free path becomes larger than the lateral dimensions of the QD, electrons can be viewed semiclassically as billiard balls. Depending on the geometrical symmetries of the QD, they can either follow stable periodic orbits, probe particular trajectories between the entrance and exit point contacts, or be reflected back into the entrance point contact. These classical ballistic effects can be predicted semiclassically or quantum mechanically and lead to large fluctuations of the magnetoconductance:²⁻⁵ as the magnetic field is swept, the configuration of stable trajectories is modified, which affects the transmission through the QD.

On the other hand, electron decoherence is mainly probed thanks to the emergence of two quantum corrections to the magnetoconductance, weak localization (WL) and universal conductance fluctuations (UCFs), arising from quantum interferences between trajectories inside the QD. As interferences only occur when phase coherence is maintained over the trajectory length, WL and UCFs give also access to the measurement of the electron phase-coherence time τ_ϕ .⁶⁻⁹ In GaAs/AlGaAs open QDs, it was shown^{10,11} that the dephasing rate τ_ϕ^{-1} is the sum of two electron-electron (e-e) scattering rates: a large energy-transfer scattering mechanism with a rate τ_{ee}^{-1} , and a small energy-transfer (Nyquist) mechanism with a rate τ_N^{-1} . The temperature dependence of τ_ϕ^{-1} was found to be *qualitatively* consistent with the theoretical expression established for disordered two-dimensional (2D) electron systems:^{10,12,13}

$$\frac{1}{\tau_\phi} = \frac{1}{\tau_{ee}} + \frac{1}{\tau_N} = \frac{\pi}{2} \frac{kT^2}{\hbar E_F} \ln \frac{E_F}{kT} + \frac{kT}{2\pi\hbar} \frac{\lambda_F}{l_\mu} \ln \frac{\pi l_\mu}{\lambda_F}, \quad (1)$$

where E_F is the Fermi energy, λ_F is the Fermi wavelength, and l_μ is the mean free path. However, a *quantitative* agreement with experimental data was only found for an arbitrary value of l_μ , one order-of-magnitude smaller than l_μ measured in the two-dimensional electron gas (2DEG). At very

low temperatures, $\tau_\phi(T)$ deviates from the above temperature dependence and an unexplained saturation of τ_ϕ is observed.^{11,14}

In the present work, we analyze magnetoconductance fluctuations arising from both phase-coherent and classical focusing effects in an InGaAs/InAlAs open circular QD over a wide temperature range (from 1.3 to 204 K). τ_ϕ is extracted up to 18 K from the amplitude of UCFs. We find that $\tau_\phi(T)$ agrees quantitatively with the temperature dependence predicted for the dephasing time in disordered 2D electron systems. Moreover, the absolute value of τ_ϕ is two to four times larger in our sample than in GaAs/AlGaAs QDs. This enhancement is explained using the 2D model of e-e interactions and taking into account the larger electron density and the smaller electron effective mass in InGaAs, and using the value of l_μ measured in the 2DEG.

We measured the magnetoconductance of a ballistic quantum dot, fabricated on a δ -doped InGaAs/InAlAs heterostructure using electron-beam lithography and wet etching. A schematic layer sequence of the heterostructure is shown in Fig. 1. At low temperature, the electron surface density in the substrate is $n = 9.7 \times 10^{11} \text{ cm}^{-2}$ and the mobility $\mu \sim 3 \times 10^4 \text{ cm}^2/\text{Vs}$, equivalent to $l_\mu \sim 500 \text{ nm}$. n is calculated from the Shubnikov-de Haas effect measured on a 500-nm-wide Hall bar patterned next to the cavity. Note that the effect becomes significant above 2 T. The dot has a circular shape, with a lithographic diameter of 430 nm and opening widths of 65 nm. The depletion length at device edges is $\sim 25 \text{ nm}$. Therefore, the *real* diameter and opening widths are, respectively, 380 nm and 15 nm. A metallic gate deposited on the whole structure allows one to simultaneously tune its shape and change the electron density. The measurements were performed at temperatures between 1.3 K and 204 K, using a standard lock-in technique with less than 1 nA bias current below 83 K and less than 10 nA above. In those ranges, the magnetoconductance was found to be current independent.

Figure 1 shows the magnetoconductance $G(B)$ of the nanocavity at different temperatures, with the gate grounded. The mean conductance $\langle G \rangle$ of the cavity slightly increases

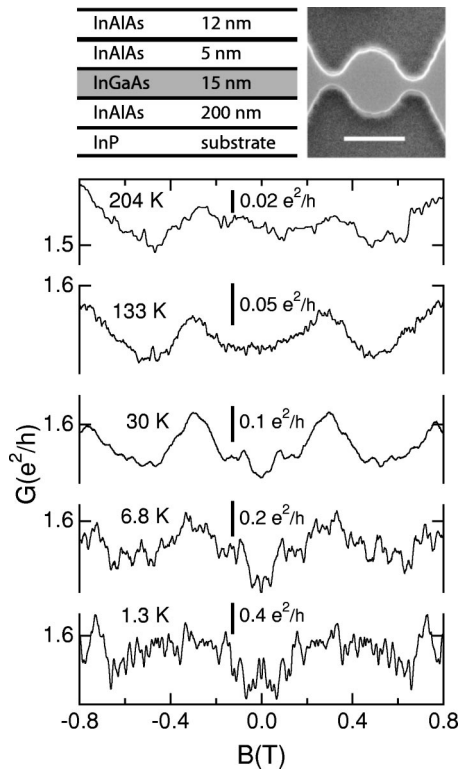


FIG. 1. Top left: Layer sequence of the heterostructure. The 2DEG is located in the gray layer, and the delta-doped layer is the bold line. Top right: Electron micrograph of the device. Darker regions are etched. The white bar represents 430 nm. Bottom: Magnetoconductance of the quantum dot at indicated temperatures. Notice the different conductance scales on top of each trace.

with temperature from $\sim 1.4 e^2/h$ at 1.3 K to $\sim 1.52 e^2/h$ at 12 K and remains constant at higher temperature. This means that the number of channels N_1 and N_2 in each point contact is between 1 and 2. We therefore assume a total number of channels $N = N_1 + N_2 = 3$. Below 12 K, the temperature dependence of the maxima and minima in $G(B)$ is mainly consistent with previous works.¹⁵ The magnetoconductance traces in Fig. 1 show the superposition of two distinct types of reproducible conductance fluctuations with different temperature dependencies, both symmetric with respect to $B = 0$. The first ones, also called UCFs, are related to electron interference phenomena inside the dot. Their characteristic magnetic-field scale is ~ 0.01 to 0.1 T. They persist up to 30 K, much higher than previous experiments on open QDs fabricated from AlGaAs/GaAs heterostructures.^{1,10,11} Recently, measurements on a 25-nm InGaAs quantum wire demonstrated a persistence of UCFs up to ~ 10 K.¹⁶ The amplitude of the second type of fluctuation decreases even more slowly, since they are still visible at 204 K, our highest measurement temperature. Their characteristic magnetic-field scale is ~ 0.5 T.

We first discuss these high-temperature fluctuations. From simple classical and geometrical arguments, one can calculate the magnetic field corresponding to the main trajectories inside the cavity using the expression of r_c , the cyclotron radius:³ $r_c = \hbar(2\pi n)^{1/2}/eB$. One expects a conductance

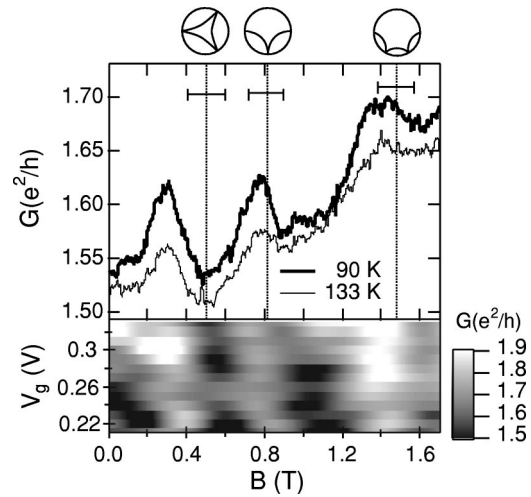


FIG. 2. Top: $G(B)$ at high temperature in our dot, with positions of classical trajectories inside the cavity. Bottom: color plot of G as a function of B and V_g at low temperature (Ref. 17).

maximum for trajectories linking both point contacts and a minimum for paths leading to electron reflection back into the entrance point contact. Figure 2 shows the agreement between the magnetic fields calculated for the expected trajectories and the maxima and minima in the magnetoconductance. The error bars on the graph take into account the uncertainty about the electron density and the depletion length. Note that we have assumed only one direction for carrier injection inside the cavity. A more realistic picture would take into account an injection cone, which effectively widens the peaks. These maxima and minima are also robust with respect to changes of the gate voltage V_g , as shown in Fig. 2.^{17,18} This confirms that these fluctuations are very different from UCFs, which are much more sensitive to small changes of E_F . The maxima at $B = 0.81$ T and 1.47 T correspond, respectively, to a trajectory length $L_e \sim 596$ nm and 700 nm, both larger than l_μ , even at low temperature. However, it was shown¹⁹ that ballistic effects can still be observed when $L_e \geq l_\mu$. A more detailed analysis of these fluctuations is presented elsewhere.²⁰

Next, the analysis of UCFs enables us to extract the phase-coherence time τ_ϕ . In previous experiments on QDs, τ_ϕ was determined either from the magnetic-field dependence of UCFs in the edge-state regime,¹⁴ or by measuring the weak-localization peak height or width,^{10,11} after averaging over a large number of magnetoconductance traces corresponding to different dot shapes (in order to reduce the UCFs amplitude). Since in our sample, V_g also changes the electron density, we use another procedure based on the measurement of UCFs variance, which was shown to be equivalent to the weak-localization method.²¹ In this approach, the variance of UCFs is related to τ_ϕ with an approximated expression, strictly valid if $\Delta \ll kT$ where $\Delta = 2\pi\hbar^2/m^*A_{dot}$ is the mean energy-level spacing inside the dot ($m^* = 0.042m_0$ is the electron effective mass, and $A_{dot} = 0.113 \mu\text{m}^2$ is the area of the dot). In our case, $\Delta/k \sim 1.2$ K, which is comparable to our lowest measurement temperature. Therefore, we have to use the following gener-

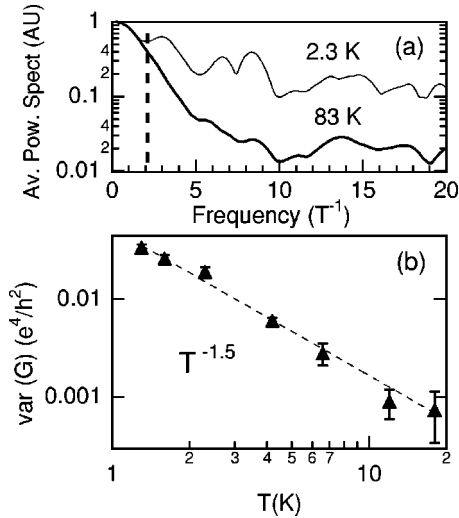


FIG. 3. (a) Average power spectrum of conductance fluctuations at 2.3 and 83 K, in arbitrary units. The dashed line corresponds to the cutoff frequency f_c (see text). (b) $\text{var}(G)$ as a function of T , in units of e^4/h^2 , evaluated in the range $0.3 T < B < 1 T$. The dashed line is a fit to a $T^{-1.5}$ law.

alized formula for the variance of UCFs, $\text{var}(G)$, including dephasing and thermal averaging:⁹

$$\text{var}(G) = \int_0^\infty \int_0^\infty f'(E)f'(E')\text{cov}(E,E')dEdE', \quad (2)$$

where E and E' are energies, $f'(E)$ is the derivative of the Fermi function, $\text{cov}(E,E') = \langle G \rangle^2 / [(N + N_\phi)^2 + 4\pi^2(E - E')^2/\Delta^2]$ is the conductance correlator, and $N_\phi = 2\pi\hbar/(\tau_\phi\Delta)$.

Before evaluating $\text{var}(G)$, UCFs must be separated from the slowly varying background of ballistic fluctuations discussed above. In order to identify the contribution of these slow fluctuations to $G(B)$, we compare the power spectrum (PS) of $G(B)$ at low temperature (2.3 K) and at high temperature (83 K), where UCFs have disappeared [Fig. 3(a) (Ref. 22)]. At low frequencies ($\leq 2 T^{-1}$), the PS is clearly temperature independent, and strongly depends on T at higher frequencies ($\geq 2 T^{-1}$). Therefore, $\text{var}(G)$ is evaluated from high-pass filtered $G(B)$ traces, with a cutoff frequency $f_c = 2 T^{-1}$. Figure 3(b) shows that $\text{var}(G)$ follows a $\sim T^{-1.5}$ law. The uncertainty over $\text{var}(G)$ grows with T , as $\text{var}(G)$ becomes comparable to the amplitude of the slowly varying background at 20 K. Note that $\text{var}(G)$ is evaluated in the range $0.3 T < B < 1 T$, so that r_c is larger than the cavity radius, and time-reversal symmetry is broken ($B > \phi_0/A_{dot}$, where ϕ_0 is the quantum of magnetic flux).

Figure 4 shows the temperature dependence of τ_ϕ , extracted from $\text{var}(G)$ using a numerical evaluation of Eq. (2). The error bars on τ_ϕ take into account the uncertainty about $\text{var}(G)$, N , Δ , and $\langle G \rangle$. We observe a good quantitative agreement between the measured $\tau_\phi(T)$ and the theoretical prediction for e-e scattering in a diffusive 2D system, i.e., Eq. (1), with $E_F = \hbar^2 \pi n / m^* = 55.3$ meV, $l_\mu = 500$ nm, and $\lambda_F = 16$ nm (dashed line in Fig. 4). Note that Eq. (1) does not have any adjustable parameters. We do not observe any sig-

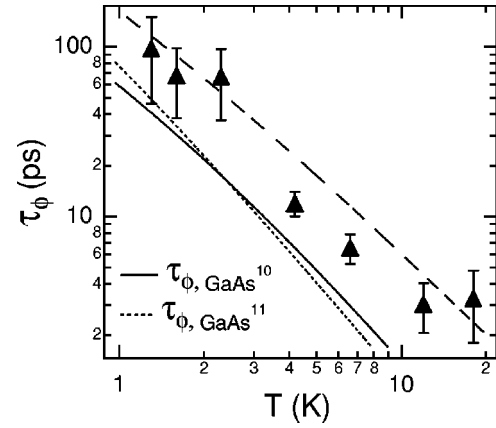


FIG. 4. Triangles: τ_ϕ vs T in our InGaAs sample. Dashed line: theoretical $\tau_\phi(T)$ in InGaAs, predicted using Eq. (1). Solid and dotted lines: fits to experimental values of $\tau_\phi(T)$ found for GaAs quantum dots (Refs. 10 and 11).

nificant departure from the model (1) in our temperature range. Hence, dephasing is fully determined by e-e interactions, and electron-phonon scattering is negligible even at 20 K (in 2D samples, a rate $\tau_\phi^{-1} \propto T^3$ is expected when electron-phonon interaction dominates²³).

Figure 4 also compares our data to the electron dephasing time in GaAs quantum dots.^{10,11,24} The temperature dependence of τ_ϕ is clearly similar in both types of QDs. One can therefore reasonably conclude that dephasing is governed by the same scattering mechanisms in both types of QDs. However, $\tau_\phi(T)$ is approximately two to four times larger in our InGaAs/InAlAs structure. In order to explain the origin of the enhancement of τ_ϕ in our QD, we have gathered the main parameters of our sample in Table I, along with the data on GaAs QDs.^{10,11} In the same way as Huibers and co-workers,^{10,11} we performed a fit of the form $\tau_\phi^{-1}(T) = aT + bT^2$ to our data, where a and b are constants²⁵ [this is an approximated form of Eq. (1)]. The coefficient of the T^2 term is a factor of 6–9 smaller in InGaAs QDs than in GaAs/AlGaAs QDs, while the coefficient of the T term varies only by a factor of ~ 2 –3 among the various samples. The difference in the coefficient of the T^2 term can be explained by the larger E_F in our sample [see Eq. (1)], originating from a smaller m^* and a larger n . This explains the larger value of τ_ϕ in our sample,²⁶ and further demonstrates the validity of the 2D diffusive model of e-e interactions [Eq. (1)] in the case of open QDs. Note that, around 1 K, τ_ϕ in our InGaAs QD becomes closer to the τ_ϕ given in Ref. 11. In this range, τ_ϕ is dominated by the T term, which depends on the ratio λ_F/l_μ . Table I clearly shows that this ratio in our sample is indeed very close to that in Ref. 11.

In summary, we have evidenced classical ballistic focusing effects up to 204 K in the magnetoconductance of an open InGaAs quantum dot. We have also measured the electron dephasing time τ_ϕ up to 18 K using the variance of universal conductance fluctuations. We find that $\tau_\phi(T)$ is *quantitatively* consistent with the temperature dependence predicted in 2D disordered systems. Furthermore, τ_ϕ in our sample is larger than in GaAs/AlGaAs quantum dots

TABLE I. Summary of relevant transport parameters for InGaAs and GaAs QDs, with the experimental fits to $\tau_\phi(T)$.

	InGaAs	GaAs ^a	GaAs ^b
m^* ($*m_0$)	0.042	0.067	0.067
$n(10^{15} \text{ m}^{-2})$	9.7	2	1.8
l_μ (nm)	500	1500	6000
A_{dot} (μm^2)	0.113	8–1.6	4–0.4
Δ (μeV)	90.6	0.8–4	1.8–17.9
E_F (meV)	55.5	7.15	6.44
λ_F/l_μ	0.05	0.037	0.01
τ_ϕ^{-1} (ns^{-1})	$5(\pm 2)T + 1.1(\pm 0.3)T^2$	$4T + 9T^2$	$10.9T + 6.1T^2$

^aReference 11.^bReference 10.

by a factor of 2–4, which we explain by a larger Fermi energy. Our results therefore demonstrate that, at low temperature, τ_ϕ can easily be enhanced by controlling n , m^* , and l_μ .

The authors acknowledge P.W. Brouwer for providing valuable information. B.H., S.F., and C.G. acknowledge financial support from the Fonds de Recherche pour

l'Industrie et l'Agriculture (F.R.I.A.). This work was also supported by the PAI - IUAP program of the Belgian Government and by the "Action de Recherche Concertée" of the "Communauté Française de Belgique." This work has also been partially supported by the European Commission through the European Commission through the NANOTERA project IST-2001-32517.

¹C.M. Marcus *et al.*, Phys. Rev. Lett. **69**, 506 (1992).²J.P. Bird *et al.* Europhys. Lett. **35**, 529 (1996).³H. Linke, L. Christensson, P. Omling, and P.E. Lindelof, Phys. Rev. B **56**, 1440 (1997).⁴P. Bøggild, A. Kristensen, and P.E. Lindelof, Phys. Rev. B **59**, 13 067 (1999).⁵P. Bøggild *et al.*, Phys. Rev. B **57**, 15 408 (1998).⁶H.U. Baranger and P.A. Mello, Phys. Rev. B **51**, 4703 (1995).⁷P.W. Brouwer and C.W.J. Beenakker, Phys. Rev. B **51**, 7739 (1995).⁸K. Efetov, Phys. Rev. Lett. **74**, 2299 (1995).⁹K. Frahm, Europhys. Lett. **30**, 457 (1995).¹⁰A.G. Huibers *et al.*, Phys. Rev. Lett. **81**, 200 (1998).¹¹A.G. Huibers *et al.*, Phys. Rev. Lett. **83**, 5090 (1999).¹²B.L. Altshuler, A.G. Aronov, and D.E. Khmel'nitsky, J. Phys. C **15**, 7367 (1982).¹³K.K. Choi, D.C. Tsui, and K. Alavi, Phys. Rev. B **36**, 7751 (1987).¹⁴D.P. Pivin, A. Andresen, J.P. Bird, and D.K. Ferry, Phys. Rev. Lett. **82**, 4687 (1999).¹⁵A. Shailos *et al.*, Phys. Rev. B **63**, 241302 (2001); **64**, 193302 (2001).¹⁶T. Sugaya *et al.*, Appl. Phys. Lett. **80**, 434 (2002).¹⁷The colorplot in Fig. 2 is obtained from low-pass filtered $G(B)$ traces with a cutoff frequency 3 T^{-1} .¹⁸Note that the change in n caused by the sweep of V_g from 0 V to 0.33 V only induces a difference of $\sim 1\%$ of r_c , which cannot be detected in our measurement.¹⁹Y. Hirayama and S. Tarucha, Appl. Phys. Lett. **63**, 2366 (1993).²⁰B. Hackens *et al.*, cond-mat/0210093 (unpublished); Physica E (to be published).²¹A.G. Huibers *et al.*, Phys. Rev. Lett. **81**, 1917 (1998).²²Spectra in Fig. 3(a) are averages of three fast Fourier-transform power spectra from half-overlapping blocks in the range $0.3 \text{ T} < B < 4 \text{ T}$.²³A. Mittal *et al.*, Surf. Sci. **361/362**, 537 (1996).²⁴The experimental fits for τ_ϕ in GaAs/AlGaAs QDs (Fig. 4) are extrapolated up to 10 K for comparison purposes: the data were measured in the range $0.03 \text{ K} < T < 4 \text{ K}$.²⁵The error over the coefficient of the T term is large compared to the error over the coefficient of the T^2 term, because the T^2 term dominates the dephasing rate in the major part of our temperature range (it is larger than the T term above $\sim 4 \text{ K}$ in InGaAs QDs, and above $\sim 1 \text{ K}$ in GaAs QDs).²⁶As evidenced by Huibers and co-workers (Refs. 10 and 11) variations of N and Δ do not influence $\tau_\phi(T)$. Therefore the enhancement of τ_ϕ cannot be related to the larger value of these parameters in our sample.